Optical and mechanical properties in photorefractive crystal based ultrasound-modulated optical tomography

Huiliang Zhang, Xiao Xu, De-Kui Qing, Philip Hemmer, Lihong V. Wang

Huiliang Zhang, Xiao Xu, De-Kui Qing, Philip Hemmer, Lihong V. Wang, "Optical and mechanical properties in photorefractive crystal based ultrasound-modulated optical tomography," Proc. SPIE 6086, Photons Plus Ultrasound: Imaging and Sensing 2006: The Seventh Conference on Biomedical Thermoacoustics, Optoacoustics, and Acousto-optics, 608616 (6 March 2006); doi: 10.1117/12.646155

SPIE.

Event: SPIE BiOS, 2006, San Jose, California, United States

Optical and mechanical properties in photorefractive crystal based ultrasound-modulated optical tomography

Huiliang Zhang,[a] Xiao Xu,[b] De-Kui Qing,[c]
Philip Hemmer[a] and Lihong V. Wang[b]

a, Department of Electrical and Computer Engineering,
Texas A&M University, College Station, TX, 77843
b, Optical Imaging Laboratory, Department of Biomedical Engineering,
Texas A&M University, College Station, TX, 77843
c, Institute for Quantum Studies and Department of Physics,
Texas A&M University, College Station, TX, 77843

ABSTRACT

Ultrasound-modulated optical tomography (UOT) is a new technique that combines laser light and ultrasound to provide images with good optical contrast and good ultrasound resolution in soft biological tissue. We improve the method proposed by Murray *et al* to obtain UOT images in thick biological tissues with the use of photorefractive crystal based interferometers. It is found that a long ultrasound burst (on the order of a millisecond) can improve the signal-to-noise ratio dramatically. Also with a long ultrasound burst, the response of the acoustic radiation force impulses can be clearly observed in the UOT signal, which will help to acquire images that record both the optical and mechanical properties of biological soft tissues.

Keywords: ultrasound-modulated optical tomography, photorefractive, acoustic radiation force

1. INTRODUCTION

In the past decade, a great deal of effort has been expended on attempting to develop optical techniques for imaging soft biological tissues. The critical task has been to improve the unsatisfactory resolution that is caused by the strong scattering of light within biological tissues, especially at imaging depths where light is completely diffusive. Ultrasound-modulated optical tomography (UOT)[1,2] is a promising method because it combines both ultrasonic resolution and optical contrast by phase modulating or by tagging diffusive light with ultrasonic frequencies. For example, Marks *et al*.[1] first investigated the possibility of tagging light with ultrasound. Wang *et al*.[2] developed UOT and obtained images of buried samples in tissue-mimicking phantoms with *cw* ultrasound and *cw* laser light. This work was followed by Kempe *et al*.[3] In 1999, Leveque *et al*.[4] reported a parallel speckle detection scheme to improve the signal-to-noise ratio (SNR) by using a source-synchronized lock-in technique with a charge coupled device (CCD) used as a detector array. Where N is the number of pixels of the CCD, this method improved the SNR $N^{1/2}$ times over single-detector schemes. However, this technique is slow and has a narrow frequency band. Therefore, it cannot detect all of the tagged "photons" when a pulsed-ultrasound is used. Recently, a long-cavity confocal Fabry-Perot interferometer, which provides a large entendue and a short response time, was used to detect UOT signals.[5] Almost at the same time, a novel technique with an interferometry system inside a photorefractive crystal (PRC) was introduced.[6-9] It is claimed[10] that this technique, which is able to detect the tagged photons with a larger entendue than CCD parallel detection, is potentially fast enough to detect all of the tagged photons in *in vivo* biological samples.

Acoustic radiation force impulse imaging (ARFI)[11, 12] is a recently developed method for imaging the elastic properties of tissue. Though acoustic radiation force has been known for a century (please see ref. 13 for a good review), it has only recently been applied to the assessment of the properties of bio-materials.[14] One big step for the application of acoustic radiation force was the emergence of 'Ultrasound-Stimulated Vibro-Acoustic Spectrography',[15] where tissue

Photons Plus Ultrasound: Imaging and Sensing 2006: The 7th Conference on Biomedical Thermoacoustics, Optoacoustics, and Acousto-optics, edited by A. A. Oraevsky, et. al
Proc. of SPIE Vol. 6086, 608616 (2006) • 1605-7422/06/$15 • doi: 10.1117/12.646155

responses to an oscillatory radiation force were produced by interference between frequency shifted focused beams of ultrasound. The first results of ARFI *in vivo* are presented in ref. 12. Compared with normal ultrasound imaging like B-mode, acoustic radiation force is particularly suitable for the noninvasive detection of hard tissue inclusions. The stiffness of soft tissues, however, is related to their composition and changes are often related to pathology or therapy. However, because ARFI uses high acoustic intensities within quite a short time span, unlike the continuous ultrasound in ref. 15, there are no obvious increases of tissue temperature. Also, ARFI has the advantage of simple alignment because the same transducer is used for both pulse generation and pulse tracking.

Here we propose to use a longer ultrasound burst, around 1 millisecond, with PRC based UOT to increase the SNR. More interestingly, we have found that an acoustic radiation force effect happens in a millisecond time region, and this effect will bring us more information for imaging. In the experiment, we used the method as proposed by Murray *et al*.[6] Compared to the method reported by F. Ramaz *et al*,[7] this technique takes advantage of the dc shift of the signal, which is associated with un-modulated light or "un-tagged photons". From the perspective of energy conservation, the decrease in the energy of the un-modulated light is equal to the increase of the energy in all modulated components.[16-19] Because of this, we have the opportunity to detect the low frequency components induced by the acoustic radiation force.

2. EXPERIMENTAL SETUP

The experimental setup is schematically shown in Figure 1. For the convenience of discussion, the following coordinate system was adopted: the Y axis was the optical axis; the Z axis was in the direction of the acoustic axis; the X axis was perpendicular to both the acoustic and the optical axes. Ultrasonic waves were generated by a focused ultrasonic transducer (Ultranlab VHP100-1-R38) with a 38 mm focal length in water and a 1 MHz central working frequency. The ultrasonic transducer was immersed in a water tank for better acoustic coupling. The peak pressure at the focus was 1.5 MPa. Since the ultrasound burst had a low duty cycle, the acoustic energy was well within the ultrasound safety limit at this frequency for tissues without well

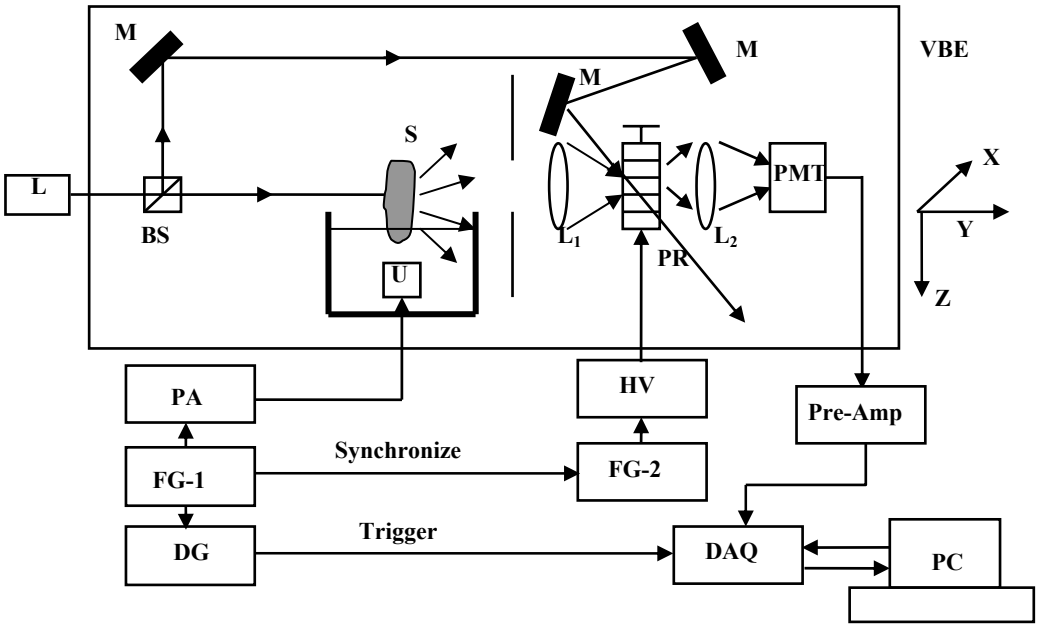

Figure 1. Schematic of the experimental setup: L, laser; BS, beam splitter; M, mirror; L_1, L_2, lens; PR, photorefractive crystal, in our case BSO; PMT, photomultiplier; FG-1, FG-2, function generator; PA, power amplifier; DG, delay-pulse generator; HV, high voltage amplifier; PC, personal computer in which data acquisition card are installed; U, 1 MHz ultrasound transducer; S, phantom sample; VBE, vibration block enclosure; DAQ, data acquisition card; Pre-Amp, pre-amplifier.

defined gas bodies.[20] The laser light (Coherent, Verdi; 532-nm) was split into two paths: one was for illuminating the sample and the other for pumping the photorefractive crystal. An aperture of 3 cm×3 cm between the sample and the first lens was used to block scattering light. The diffusive light was then collected by a lens and projected onto a photorefractive crystal (5.5×5×6 mm^3, $B_{12}SiO_{20}$), where two-wave mixing occurred between the pumping beam and the diffusive light from the sample. The BSO was selected because of its relatively large two-wave mixing gain compared with a semiconductor crystal (such as GaAs). Though the response time of the BSO, 100~200 ms in our experimental conditions, was relatively long compared with GaAs, it was still comparable to the speckle correlation time of 2 cm in the *ex vivo* chicken breast tissue[21]. To enhance the two-way mixing gain and reduce heating on the crystal,[22] a 1 KHz square wave of 8 KV/cm peak-to-peak was applied. In our experiment, the total illumination inside the crystal was typically 2 mW. Under this circumstance, we determined that the crystal response time was at least 100 ms. This fact is quite important for the assumption that the photorefractive grating remains static during the measurement period on the order of a millisecond region. A big vibration block enclosure was mounted on the optical table and covered the whole setup to protect mechanical vibration from air flow or other mechanical vibration noise sources. The first function generator (FG-1, Agilent 33250A) sent a trigger signal to a digital delay and pulse generator, DG (Stanford Research, DG535), which in turn sent a pulse to trigger a data acquisition board (Gage, CS14200). Simultaneously, the FG-1 generated a pulse train, whose length was adjusted from 1 μs to 200 ms in our experiments. After getting amplified by a power amplifier, the pulse train was used to drive the ultrasound transducer. The second function generator FG-2 shared the same time base as the FG-1. The FG-2 was also triggered by the FG-1 to generate a 1 KHz square wave, then

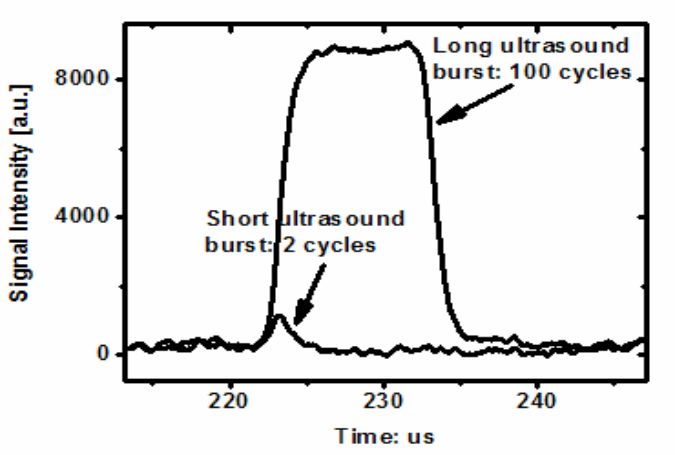

(a)

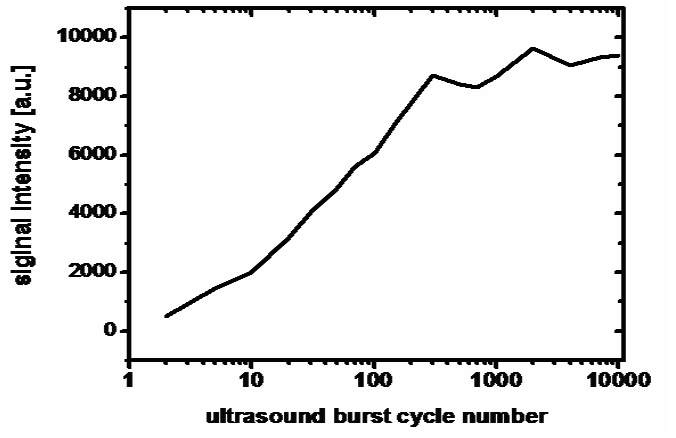

(b)

Figure 2. (a) Signal intensity comparison between the short ultrasound burst (2 cycles) and the long one (100 cycles). (b) Signal intensity changes as the burst length increases.

amplified by a high voltage amplifier, and finally applied to the photorefractive crystal. This 1 KHz high voltage square wave was always on and synchronized with the FG-2 as mentioned above.

3. RESULTS

Figure 2a shows the dramatic improvement of signal intensity (normalized modulation depth) between short ultrasound burst and long ultrasound burst. This experiment was conducted on diffusive phantoms made from water, gelatin and intralipid (Lyposine 20%) of a specific ratio in weight. The absorption coefficient was measured as $\mu_a = 0.1\ cm^{-1}$; the reduced scattering coefficient $\mu_s = 10\ cm^{-1}$. Figure 2b illustrates the change of signal intensity as a function of the number of ultrasound burst cycle. Though signal enhancement is achieved from 1 to 200 cycles, after 200 cycles, the signal appears to saturate. This happens because the longer ultrasound burst, also longer in space, induces a larger modulation area than the short one, but the effect saturates when the burst length is longer than the whole sample. Also, a longer ultrasound burst has a narrower bandwidth. Because of this reason, it is possible to eliminate the noise from other frequency band. This means SNR can be improved.

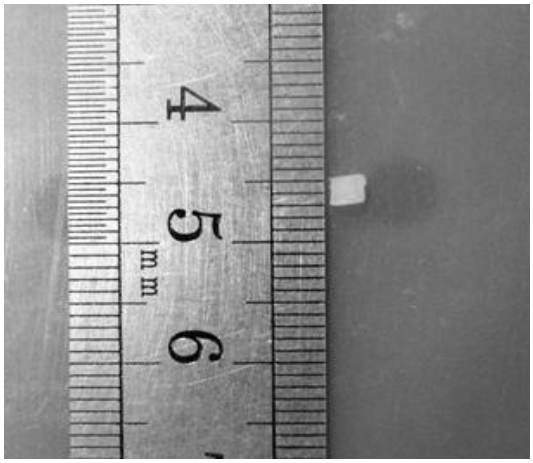

(a)

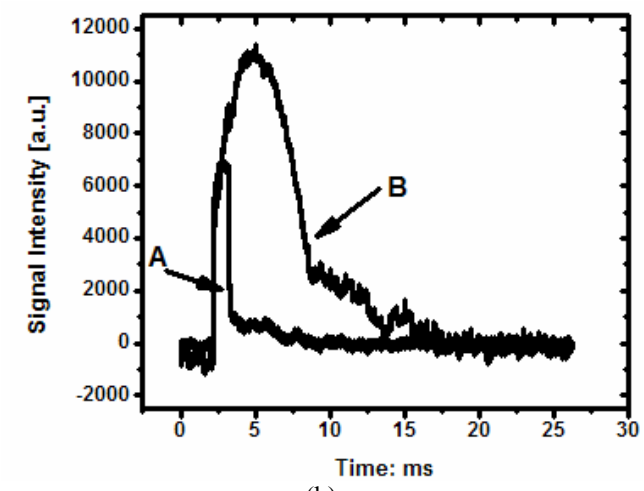

(b)

Figure 3. (a) Plastic bead, which is buried in a phantom as the imaging object. (b) Signal intensity when ultrasound is incident or not on the plastic bead.

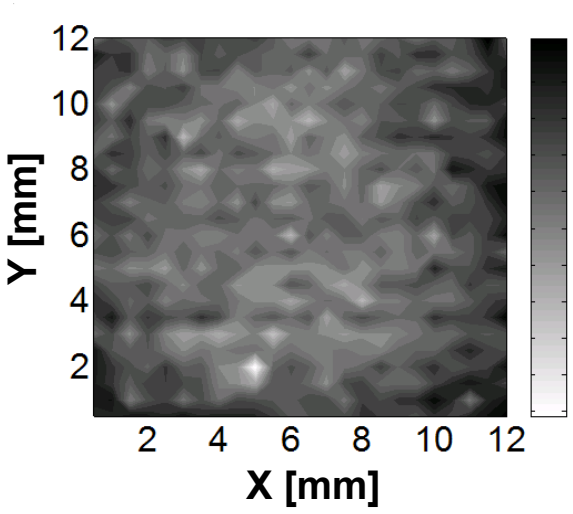

(a)

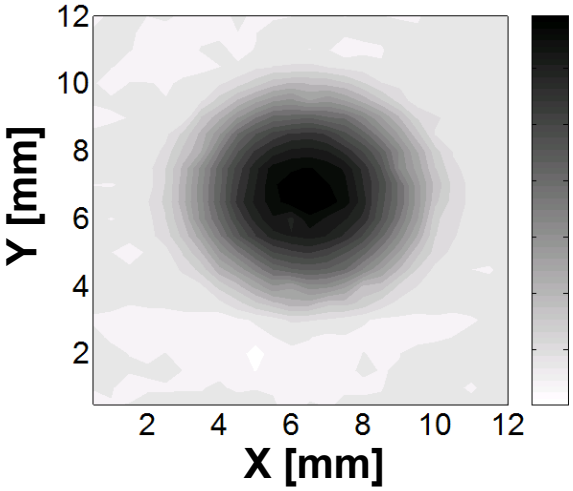

(b)

Figure 4. (a) Optical information weighted 2D image. (b) Mechanical information weighted 2D image.

A longer ultrasound burst should also give us more opportunity to observe the acoustic radiation force effect, which happens on the time order of a millisecond.[12] To verify this expectation, we buried a plastic bead, as shown in Figure 3a, inside the phantom. When the ultrasound beam was not incident on, or around, the plastic bead, the signal (line A in Figure 3b) did not show any difference from the ordinary situation. But when the ultrasound beam was incident on, or around, the plastic bead, the signal (line B in Figure 3b) was broadened and significantly increased. The time duration of the signal in line A corresponded to the ultrasound burst length. This indicates that we can still see the signal for line B even when the ultrasound has been off. The reason for this phenomenon is that the acoustic radiation force is caused by the transfer of acoustic wave momentum,[13] and it takes time for this momentum transfer to die down. This delay in time domain enables us to separate the ultrasound radiation force signal from normal UOT signal. Information about optical (absorption) properties can be obtained by averaging the output signal after the ultrasound is on within tens of microsecond. On the other hand, information about mechanical stiffness can be obtained from averaging the output signal after the ultrasound is off within tens of microseconds. In this fashion, we get two-dimensional (2D) images as shown in Figure 4. There is not much optical contrast between the plastic bead and background so Figure 4a does not show anything clearly. However, we do find a clear image for the plastic bead in Figure 4b. Here the plastic bead has a big acoustic impedance mismatch with the background phantom. When the ultrasound beam is incident on, or around,

the plastic bead, a large momentum transfer occurs because of the impedance mismatch. The acoustic radiation force tries to push the scattering particles from their original positions, which is how the phase of the light is modulated. This is only a preliminary explanation of how the acoustic radiation force effect tags the light wave; more investigation is needed in this area.

When we increase the ultrasound burst duration to tens of ms, the acoustic radiation force effect cannot be clearly distinguished from the normal signal. However, hybrid imaging with optical and mechanical information can be achieved. Also the relative weight of both information can be determined. Figure 5 shows a 2D image of chicken gizzards buried in the phantom. Chicken gizzards are the optical absorbers, but they also have mechanical properties that are different from the background. In Figure 5, the object area has a weaker signal, which means a lower modulation depth. This illustrates that optical contrast is still the dominant factor for imaging in this case, because as mentioned above, if the mechanical contrasts were dominant, we would have seen more modulation and a stronger signal in the object area. Figure 6 shows the opposite situation with the nude mouse tail buried in the phantom. The nude mouse tail does not have much optical contrast than the background, but it does have a large mechanical difference because of the bone inside. With higher modulation depth in the object area, we see a dark object in a bright background.

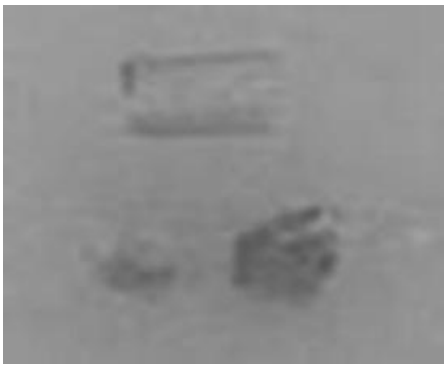

(a)

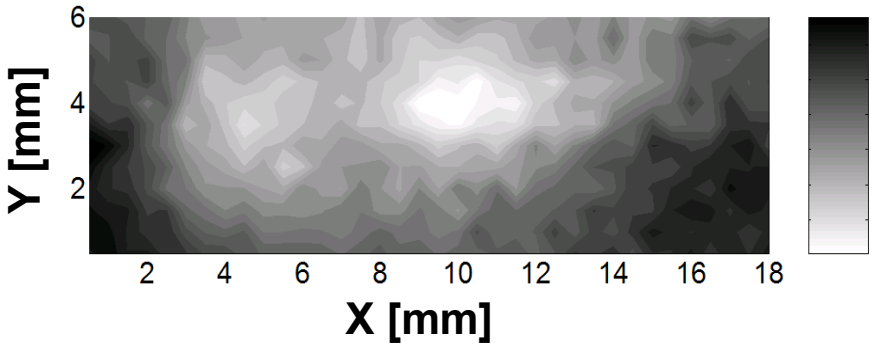

(b)

Figure 5. (a) chicken gizzards; reference bar is 5 mm. (b) 2D image for chicken gizzard buried in phantom.

4. RESULTS

In summary, we have demonstrated that in the photorefractive crystal based detection scheme of UOT, the SNR can be improved by a longer ultrasound burst. Because of the wideband frequency detection principle in this scheme, we find that the acoustic radiation force can be detected with a longer ultrasound burst in the millisecond region. In this way, the decoupling of optical and mechanical information in UOT becomes possible. The relative weight of the optical and mechanical information can also be determined by a similar method.

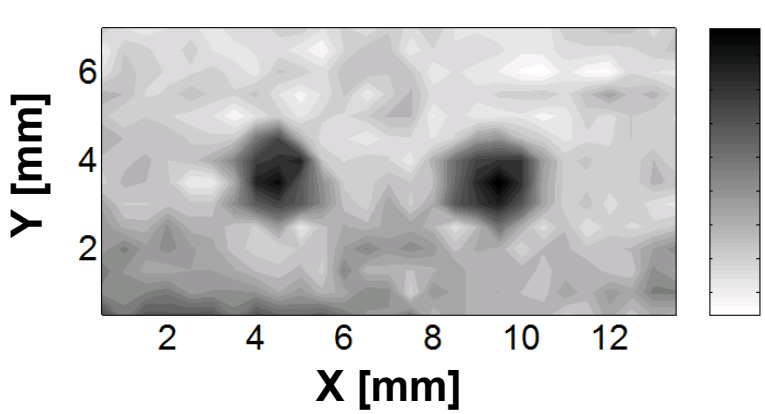

Figure 6. 2D image for nude mouse tail buried in phantom.

5. ACKNOWLEDGEMENT

We thank Chul Hong Kim for assistance with experiments measurements. We also appreciate Sava Sakadžic´ and Roger Zemp for fruitful scientific discussions. This research was supported by the National Institute of Health grant R33 CA 094267 and AFOSR FA9550-04-1-0247. L. Wang's e-mail address is lwang@tamu.edu.

REFERENCES

1. F. A. Marks, H. W. Tomlinson, and G. W. Brooksby, "A comprehensive approach to breast cancer detection using light: photon localization by ultrasound modulation and tissue characterization by spectral discrimination," *Proc. SPIE*. **1888**, pp. 500-510 (1993).
2. L. V. Wang, S. L. Jacques, and X. Zhao, "Continuous-wave ultrasonic modulation of scattered laser light to image objects in turbid media," *Opt. Lett*. **20,** pp. 629-631 (1995).
3. M. Kempe, M. Larionov, D. Zaslavsky, and A. Z. Genack, "Acousto-optic tomography with multiply scattered light," *J. Opt. Soc. Am. A*. **14**, pp. 1151-1158 (1997).
4. S. Leveque, A. C. Boccara, M. Lebec, and H. Saint-Jalmes, "Ultrasonic tagging of photon paths in scattering media: parallel speckle modulation processing," *Opt. Lett*. **24**, pp. 181-183 (1999).
5. S. Sakadzˇic´ and L. V. Wang, "High resolution ultrasound-modulated optical tomography in biological tissues", *Opt. Lett*. **29**, pp. 2770-2772 (2004).
6. T. W. Murray, L. Sui, G. Maguluri, R. A. Roy, A. Nieva, F. Blonigen, and C. A. DiMarzio, "Detection of ultrasound modulated photons in diffuse media using the photorefractive effect," *Opt. Lett*. **29**, pp. 2509-2511, (2004).
7. F. Ramaz, B.C. Forget, M. Atlan, A.C. Boccara, M. Gross, P. Delaye, G. Roosen, "Photorefractive detection of tagged photons in ultrasound modulated optical tomography of thick biological tissues," *Opt. Express*. **12**, pp. 5469-5474 (2004).
8. E. Bossy, L. Sui, T. W. Murray and R. A. Roy, "Fusion of conventional ultrasound imaging and acousto-optic sensing by use of a standard pulsed-ultrasound scanner," *Opt. Lett*. **30**, pp. 744-746 (2005).
9. F. J. Blonigen, A. Nieva, C. Dimarzio, S. Manneville, L. Sui, G. Maguluri, T. W. Murray, and R. A. Roy, "Imaging in diffuse media with pulsed-ultrasound-modulated light and the photorefractive effect," *Appl. Opt*. **44**, pp. 4041-4048 (2005).

10. M. Gross, F. Ramaz, B. C. Forget, M. Atlan, A.C. Boccara, P. Delaye, and G. Roosen, "Theoretical description of the photorefractive detection of the ultrasound modulated photons in scattering media," *Opt. Express*. **13**, pp. 7097-7112 (2005).
11. K. Nightingale, R. Nightingale, M. Palmeri and G. Tachey, "A finite element model of remote palpation of breast lesions using radiation force: factors affecting tissue displacement," *Ultrason. Imaging*. **22**, pp. 35-54 (2000).
12. K. Nightingale, M. Soo, R. Nightingale, and G. Trahey, "Acoustic radiation force impulse imaging: *in vivo* demonstration of clinical feasibility," *Ultrasound Med. Biol*. **28**, pp. 227-235 (2002).
13. G. Torr, "The acoustic radiation force", *Amer. J. Phys*. **52**, pp. 402-408 (1984)
14. T. Sugimoto, S. Ueha and K. Itoh, "Tissue hardness measurement using the radiation force of focused ultrasound," *Proceedings of the 1990 IEEE Ultrasonics Symposium*. pp. 1377-1380 (1990)
15. M. Fatemi and J. F. Greenleaf, "Ultrasound-stimulated vibro-acoustic spectrography," *Science*. **280**, pp. 82-85 (1998)
16. W. Leutz, G. Maret, "Ultrasonic modulation of multiply scattered light", *Physica B*. **204**, pp. 14-19 (1995).
17. L. V. Wang, "Mechanism of ultrasonic modulation of multiply scattered coherent light: an analytic model," *Phys. Rev. Lett*. **87**, (043903) pp. 1-4 (2001).
18. S. Sakadzˇic´ and L. V. Wang, "Ultrasonic modulation of multiply scattered coherent light: an analytical model for anisotropically scattering media," *Phys. Rev. E*. **66**, (026603) pp. 1-9 (2002).
19. S. Sakadzˇic´ and L. V. Wang, "Modulation of multiply scattered coherent light by ultrasonic pulses: An analytical model," *Phys. Rev. E*. **72**, (036620) pp. 1-12 (2005).
20. AUIM, http://www.aium.org/, *Mammalian in vivo ultrasonic biological effects*, 1992.
21. G. Yao and L. V. Wang, "Signal Dependence and Noise Source in Ultrasound-Modulated Optical Tomography," *Appl. Opt*. **43**, pp. 1320-1326 (2004).
22. P. Delaye, A. Blouin, D. Drolet, L. de Montmorillon, G. Roosen, and J. Monchalin, "Detection of ultrasonic motion of a scattering surface by photorefractive InP:Fe under an applied dc field," *J. Opt. Soc. Am. B*. **14**, pp. 1723-1734 (1997).